PROCEEDINGS OF SCIENCE

ONLINE ICRC 2021
THE ASTROPARTICLE PHYSICS CONFERENCE
Berlin | Germany
37th International Cosmic Ray Conference
12–23 July 2021

INTEGRAL X-ray constraints on sub-GeV dark matter

Marco Cirelli,[a,b] **Bradley J. Kavanagh,**[c] **Nicolao Fornengo**[d,e] **and Elena Pinetti**[a,b,d,e,*]

[a] *Sorbonne University,*
4 Place Jussieu, F-75252, Paris, France
[b] *Laboratoire de Physique Théorique et Hautes Energies (LPTHE), UMR 7589 CNRS,*
4 Place Jussieu, F-75252, Paris, France
[c] *Instituto de Fisica de Cantabria,*
Av. de Los Castros s/n, 39005 Santander, Spain
[d] *Università di Torino, Dipartimento di Fisica,*
via P. Giuria 1, I-10125 Torino, Italy
[e] *Istituto Nazionale di Fisica Nucleare, Sezione di Torino,*
via P. Giuria 1, I-10125 Torino, Italy
E-mail: elena.pinetti@unito.it

In this work we proposed to constrain sub-GeV dark matter particles (1 MeV $\leq m_{DM} \leq$ 5 GeV) by looking at energies much lower than the mass range of interest, by means of the inverse Compton scattering contribution to the total flux. In particular, the electrons and positrons produced by dark matter particles give rise to X rays by up-scattering the low-energy photons in the Milky Way, notably cosmic microwave background, infrared light from dust and optical starlight. These X rays fall in the energy range covered by the INTEGRAL data, which we used to constrain the dark matter annihilation cross-section. We considered three annihilation channels: electron, muon and pion. As a result, we derived competitive constraints for dark matter particles with a mass between 150 MeV and 1.5 GeV.

37th International Cosmic Ray Conference (ICRC 2021)
July 12th – 23rd, 2021
Online – Berlin, Germany

*Presenter

PoS(ICRC2021)563

1. Introduction

This paper is related to indirect searches of dark matter particles and is based on Ref. [1]. The dark matter (DM) in the Universe is observed to be distributed hierarchically and anisotropically on different scales: in our Galaxy, in the satellite galaxies of the Milky Way, in clusters of galaxies and in the cosmic web. If DM candidates annihilate into standard model particles, they will produce a huge variety of astrophysical messengers, which can provide invaluable information on the DM properties. In the case of sub-GeV dark matter, we expect low-energy neutrinos, sub-GeV charged cosmic rays and photons. Low-energy neutrinos are of difficult detection, due to the overwhelming solar neutrino background. Sub-GeV charged cosmic rays are deflected by the solar magnetic field, so we have no access to them, apart from the observations of the Voyager1 spacecraft outside of the heliosphere. Concerning photons, we may look for γ and X rays, as well as radio waves emitted via synchrotron emission. The additional positive aspects of neutral particles, like photons and neutrinos, is that they are not deflected by magnetic fields and therefore they trace the origin of the emitting source. However, in the sub-GeV energy range, there is a scarcity of recent measurements of the photon flux, known as the MeV gap. A few next-generation detectors, notably e-Astrogam and Amigo, have been proposed to fill this gap but none of them has been approved and funded at the time of writing. In the meanwhile, the scientific community is committed in finding alternative ways to study DM particles with a mass in the MeV range. The key idea behind our research is that sub-GeV DM can produce photons with an energy much lower than its mass, as a result of the inverse Compton scattering between DM-produced $e^{\pm}$ and the photon bath in the Milky Way.

2. The signal

In our analysis we focused on DM particles with a mass m_χ in the range

$$1 \text{ MeV} \leq m_\chi \leq 5 \text{ GeV}\,, \tag{1}$$

which annihilate into standard model particles. In particular, we considered three annihilation channels

$$\chi\chi \longrightarrow e^+e^- \tag{2}$$

$$\chi\chi \longrightarrow \mu^+\mu^- \tag{3}$$

$$\chi\chi \longrightarrow \pi^+\pi^-\,. \tag{4}$$

Each of these channels is kinematically open whenever $m_\chi > m_i$, with $i = e,\, \mu,\, \pi$. The electron and the muon channels are representative of leptonic DM channels, while the pion channel stands for an hadronic DM channel. The total DM flux that we would like to observe with our telescopes is the sum of three main contributions: final state radiation, radiative decay emission and inverse Compton scattering contribution. In the following we will explain these components one by one. Let us consider two DM particles which annihilate into muons. These secondary particles can radiate a photon, and this contribution is known as final state radiation. Alternatively, the muon can decay and emit radiative decay emission via:

$$\mu^- \longrightarrow e^-\,\bar{\nu}_e\,\nu_\mu\,\gamma \tag{5}$$

$$\mu^+ \longrightarrow e^+\,\nu_e\,\bar{\nu}_\mu\,\gamma\,. \tag{6}$$

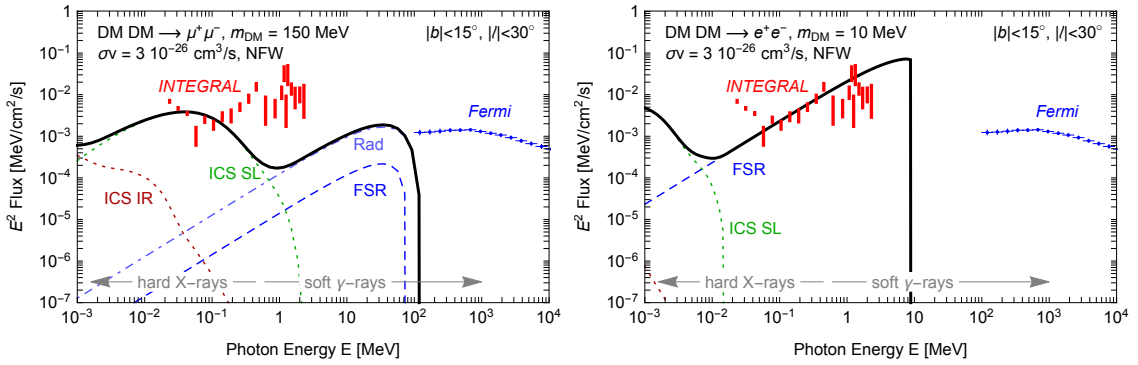

Figure 1: Photon spectra from dark matter particles with cross-section $\sigma v = 3 \cdot 10^{26}$ cm^3/s, mass of 150 MeV annihilating into $\mu^+\mu$ (left) and mass of 10 MeV annihilating into e^+e^- (right). The region of observation is $|b| < 15°, |\ell| < 30°$. The total flux is in thick black and the individual components are displayed as coloured curves: green for ICS from optical starlight, red for ICS from infrared light, dashed blue for final state radiation, dash-dotted blue for radiative decay. The red bars and blue crosses denote the INTEGRAL and FERMI data, respectively.

A similar line of argument applies also to the pions, while electrons and positrons only emit through final state radiation. Radiative decay emission (Rad) and final state radiation (FSR) constitute the so-called prompt photons. Their differential flux can be expressed as

$$\frac{\mathrm{d}\Phi_{\mathrm{prompt},\,\gamma}}{\mathrm{d}E_\gamma\,\mathrm{d}\Omega} = \frac{1}{2}\frac{r_\odot}{4\pi}\left(\frac{\rho_\odot}{m_\chi}\right)^2 J(\theta)\,\langle\sigma v\rangle_f \frac{\mathrm{d}N_\gamma^f}{\mathrm{d}E_\gamma} \tag{7}$$

where the Sun-Galactic Center distance is $r_\odot \simeq 8.33$ kpc and the local DM density is $\rho_\odot = 0.3$ GeV/cm^3. The prompt differential flux depends on the particle properties of the DM particles, notably the mass and the velocity-averaged annihilation cross section $\langle\sigma v\rangle$ in each of the final states f. Also, there is a dependence on the energy spectrum into photons $\dfrac{\mathrm{d}N_\gamma^f}{\mathrm{d}E_\gamma}$ and on the J-factor, defined as

$$J(\theta) = \int_{\mathrm{l.o.s.}} \frac{\mathrm{d}s}{r_\odot}\left(\frac{\rho\,(r\,(s,\theta))}{\rho_\odot}\right)^2 \quad \text{with} \quad \rho = \rho_s\,\frac{r_s}{r}\left(1+\frac{r}{r_s}\right)^{-2}, \tag{8}$$

where the DM halo density profile is assumed to follow a Navarro-Frenk-White profile. The two parameters $(r_s,\,\rho_s) = (24.42\ \mathrm{kpc},\ 0.184\ \mathrm{GeV/cm^3})$ are set by fixing the value of the DM density at the Sun to $\rho = 0.3$ GeV/cm^3 and the value of the total mass of our Galaxy to $M_{\mathrm{MW}} = 4.7 \cdot 10^{11}\ \mathrm{M}_\odot$. Besides the prompt photons, the DM flux includes also secondary components, notably the inverse Compton scattering (ICS) signal, which represents the key focus of our work. The electrons and positrons produced by annihilating DM can scatter the low-energy photons in our Galaxy up to X-ray frequencies. We considered three types of interstellar radiation fields (ISRF): cosmic microwave background (CMB), infrared light from dust (IR) and optical starlight (Opt). The differential flux of the ICS signal at the location $\vec{x}$ can be expressed in terms of the emissivity j as

$$\frac{\mathrm{d}\Phi_{\mathrm{ICS}\,\gamma}}{\mathrm{d}E_\gamma\,\mathrm{d}\Omega} = \frac{1}{E_\gamma}\int_{\mathrm{l.o.s.}} \mathrm{d}s\ \frac{j(E_\gamma,\vec{x})}{4\pi}\,. \tag{9}$$

The emissivity is defined as the convolution of the electron number density $n_e\,(E_e, \vec{x})$ with the power radiated into photons $\mathcal{P}_{\rm ICS}(E_\gamma, E_e, \vec{x})$ at the location $\vec{x}$

$$j(E_\gamma, \vec{x}) = 2 \int_{m_e}^{M_\chi} \mathrm{d}E_e\, \mathcal{P}_{\rm ICS}(E_\gamma, E_e, \vec{x})\, n_e\,(E_e, \vec{x})\ , \tag{10}$$

where the factor 2 denotes that annihilation events of DM particles produce an equal population of electrons and positrons. The total differential power $\mathcal{P}_{\rm ICS} = \sum_\varphi \mathcal{P}^\varphi_{\rm ICS}$ is sum over the the components of the photon bath, $\varphi \in$ [CMB, IR, Opt]. It encloses the information on the energy density of the ISRF via

$$\mathcal{P}^\varphi_{\rm IC}(E_\gamma, E_e, \vec{x}) = E_\gamma \int d\epsilon\, n_\varphi(\epsilon, \vec{x})\, \sigma_{\rm IC}(\epsilon, E_\gamma, E_e)\,, \tag{11}$$

where $\sigma_{\rm IC}(\epsilon, E_\gamma, E_e)$ represents the Klein-Nishina cross section, E_γ represents the final energy of the photons after the ICS due to $e^\pm$ with energy E_e and $n_\varphi(\epsilon, \vec{x})$ is the density of the photon bath with initial energy ϵ. We assumed the on-the-spot approximation, neglecting the diffusion of $e^\pm$. Under this assumptions, the expression of the electron number density reads

$$n_e\,(E_e, \vec{x}) = \frac{1}{b_{\rm tot}\,(E_e, \vec{x})} \int_{E_e}^{m_\chi} \mathrm{d}\tilde{E}_e\, Q_e\left(\tilde{E}_e, \vec{x}\right)\ , \tag{12}$$

where the injection term of $e^\pm$ from annihilating DM is given by

$$Q_e(\tilde{E}_e, \vec{x}) = \frac{\langle\sigma v\rangle}{2} \left(\frac{\rho(\vec{x})}{m_\chi}\right)^2 \frac{\mathrm{d}N_{e^\pm}}{\mathrm{d}\tilde{E}_e}\ . \tag{13}$$

The energy losses $b_{\rm tot}$ include ionization, bremsstrahlung, ICS, synchrotron processes: $b_{\rm tot}(E, \vec{x}) \equiv -\frac{\mathrm{d}E}{\mathrm{d}t} = b_{\rm Coul+ioniz} + b_{\rm brem} + b_{\rm syn} + b_{\rm ICS}$. The density of the ISRF and the energy losses are computed withih PPPC [8]. Thus, the differential flux in the region of interest, identified with the galactic coordinates (b, ℓ), reads

$$\frac{\mathrm{d}\Phi_{\rm Tot}\,\gamma}{\mathrm{d}E_\gamma} = \int_{b_{\rm min}}^{b_{\rm max}} \int_{\ell_{\rm min}}^{\ell_{\rm max}} \mathrm{d}b\,\mathrm{d}\ell\,\cos b\,\left(\frac{\mathrm{d}\Phi_{\rm prompt,\,\gamma}}{\mathrm{d}E_\gamma\,\mathrm{d}\Omega} + \frac{\mathrm{d}\Phi_{\rm ICS\,,\gamma}}{\mathrm{d}E_\gamma\,\mathrm{d}\Omega}\right). \tag{14}$$

Fig. 1 illustrates the energy flux as a function of the final photon energy in the rectangular region $|b| < 15°, |\ell| < 30°$, which includes the Galactic Plane. For illustrative purposes, the Fermi and Integral data are also displayed. In the left panel, the total DM signal (black line) refers to the prediction of the flux produced by DM particles with mass of 150 MeV and $\langle\sigma\, v\rangle = 3 \cdot 10^{26}$ cm^3/s, annihilating into $\mu^+\mu^-$. In this specific case, the DM flux goes undetected by the Fermi telescope, instead it overlaps with the Integral data, as a result of including the ICS on optical starlight. It is noteworthy that both the FSR and Rad pass well below the Integral meausurements and they are several order of magnitude lower than the ICS. Thus, including the ICS components proves to be pivotal for large DM masses. Instead, for low DM masses with a mass of 10 MeV, annihilating into $e^\pm$ (right panel), the leading contribution to the total flux in the energy range of Integral comes from the FSR.

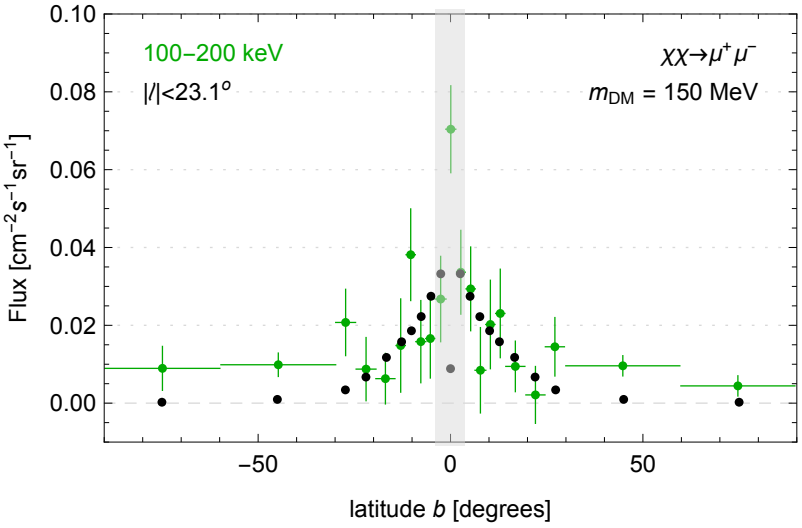

Figure 2: Angular flux as a function of the latitude bins in the longitude window $|\ell| < 23.1°$ for the energy band 100−200 keV. The INTEGRAL data are in green, while the black dots refer to the forecast of the flux for DM particles with m_χ =150 MeV, $\sigma v \approx 1.2 \cdot 10^{-26}$ cm^3/s, annihilation into $\mu^+\mu^-$.

3. Results

The INTEGRAL space telescope was an European Space Agency mission operating between 2003 and 2009. The onboard spectrometer (SPI) measured photons in the energy range 20 keV < E_γ < 8 MeV. The data are provided as an energy spectrum in a region that includes also the Galactic pùPlane and as an angular flux in latutide bins. We chose to consider the latter because it allows us to exclude the region around the Galactic Center and focusing on higher latitudes where the ICS is the prevalent type of interaction for the $e^\pm$. The data that we employed are divided in five energy bands: 27−49 keV, 49−90 keV, 100−200 keV, 200−600 keV, 600−1800 keV. Fig. 2 illustrates the angular flux as a function of the latitude for the energy band 100−200 keV. The green points refer to the INTEGRAL data, while the black points refer to our prediction of the angular flux for DM particles with a mass of 150 MeV, cross-section on our bound (see below the constraints), annihilating into $\mu^+\mu^-$. The DM flux becomes larger as we approach the central bins as a result of the larger DM density as we comes closer to the centre of the Milky Way. However, the most central latitude bin is much lower with respect to the neighbouring ones because it corresponds to lines of sight crossing the Galactic Plane, where the $e^\pm$ loose energy mostly via interaction with the interstellar gas and therefore the ICS signal is suppressed. To avoid the Galactic Plane, we mask the central latitude bins (grey stripe).

We obtain two types of constraints: conservative and optimistic. The former are derived by requiring that the predicted DM flux $\Phi_{\rm DM}$ does not exceed the measured flux ϕ by more than 2σ. In particular, we defined the text statistic

$$\chi^2_{\rm cons} = \sum_{\rm bands} \sum_{i \in \{\rm b\ \ bins\}} \frac{\left(\max\left[(\Phi_{{\rm DM},i}(\langle\sigma v\rangle) - \phi_i), 0 \right] \right)^2}{\sigma_i^2} \tag{15}$$

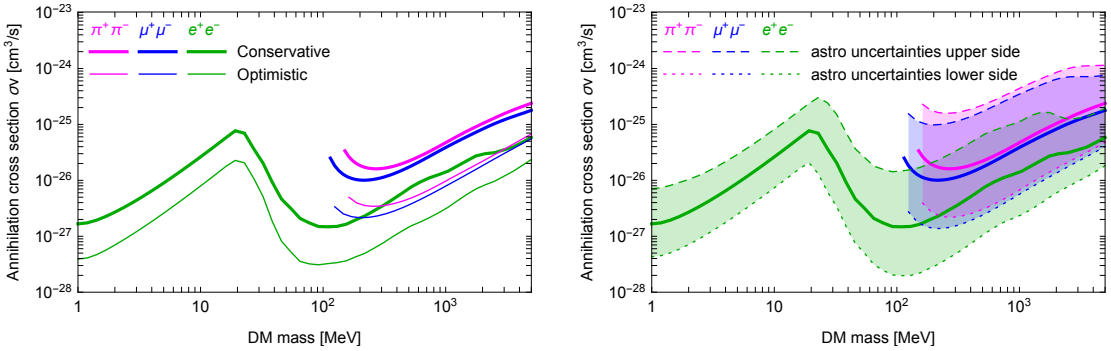

Figure 3: . *Left*: Constraints on the annihilation cross-section with and without astrophysical background (thin and thick lines, respectively). *Right*: Variation of the bounds due to the astrophysical uncertainties.

corresponding to an effective χ^2, where the first sum is performed over the energy band and the second sum over the latitude bins. By scanning over the DM masses, this statistic is equivalent to a $\Delta\chi^2$ with one degree of freedom (the annihilation cross-section). We imposed our 2σ constraints on $\langle\sigma v\rangle$ by demanding $\Delta\chi^2 = 4$. To compute these constraints we are assuming that the observed flux can be entirely explained with a DM contribution. In the real world we know that a large part of the signal will be produced by the astrophysical background. The main type of astrophysical backgorund consists of diffusive ICS. Indeed, astrophysical sources such as supernova rementants or active galatic nuclei can produce $e^{\pm}$ that undergo ICS and mimic the DM signal. Ref. [9] provides a template of the background flux ϕ_B. To obstain the constraints on the DM parameters space, we multiply ϕ_B by an overall normalization factor N_B and we adopt the following test statistic:

$$\chi^2_{\rm opt} = \sum_{\rm bands} \sum_{i\in\{\rm b\ \ bins\}} \frac{\left[\Phi_{\chi\, i}\ (\langle\sigma v\rangle) + N_B\,\phi_B - \phi_i\right]^2}{\sigma_i^2}\,. \tag{16}$$

We identify the pair $\left(N_{B,0},\ \langle\sigma v\rangle_0\right)$ that minimizes the test statistic, corresponding to the value χ_0. Thereafter, for each DM mass we scan the values of $(N,\ \langle\sigma v\rangle)$ and we constraint $\langle\sigma v\rangle$ by demanding $\Delta\chi^2 = \chi^2 - \chi^2_0 = 4$, for any N_B. It is apparent that considering an astrophysical background will leave less room for exotic physics, Thus, if we add the DM contribution on top of the background we find stronger constraints. Fig. 3 (left) display the bounds on $\langle\sigma v\rangle$ as a function of the DM mass for the three annihilation channels (electron in green, muon in blue, pion in magenta). The conservative limits are in thick lines. The optimistic bounds improve of O(60%) but they suffer of additional source of uncertainties since the astrophysical background is not fully understood. Therefore, we prefer to consider the conservative constraints as our reference bounds. It is also essential to estimate of the impact of the uncertainties on our reference constraints. In order of importance, the main sources of uncertainty are: the DM halo profile, the density of the gas, the density of the ISRF and the galactic magnetic field. The choice of the DM profile affects all three components of the total flux. We considered three different profiles: Navarro-Frenk-White (NFW, our reference case), Burkert, cusped. This choice could affect the constraints up to O(60%). The ICS signal depends on the gas and photon density. We considered a variation of a factor 2 in the density normalization, both for the insterstellar gas and ISRF. This affects the bounds less than 25%. The model of the galactic magnetic field has an impact on the synchrotron losses, which however are subdominant

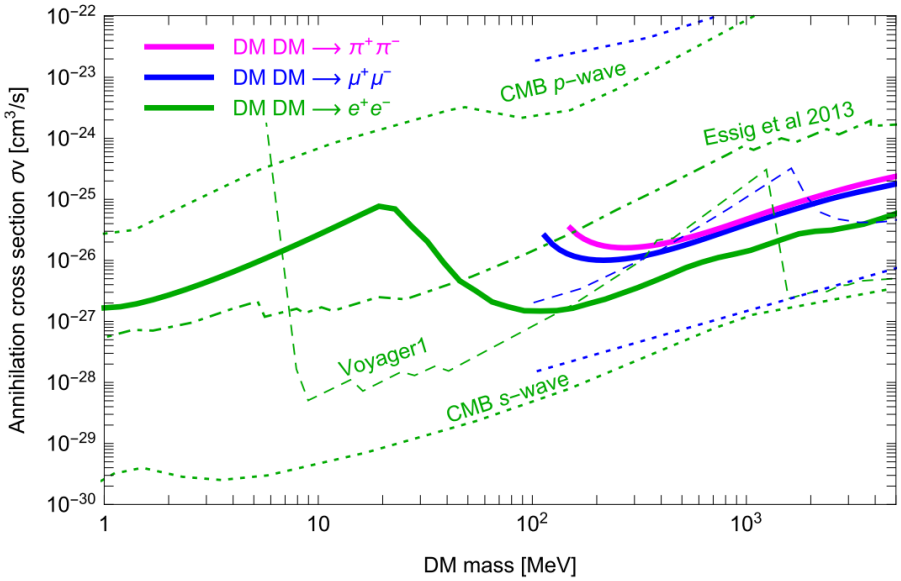

Figure 4: Our conservative constraints on the annihilation cross-section for sub-GeV DM, using the INTEGRAL data (solid thick lines). The other curves refer to the existing bounds in the literature from other probes. See the text for further details.

with respect to the other loss processes under consideration. We considered three configuration of the magnetic field in our Galaxy and the impact on the bounds is less than 30%. The variation of the constraints due to the uncertainties discussed above is illustrated in Figure 3 (right). The upper and lower sides are related to the most pessimistic and most optimistic combination of parameters entering the computation, respectively. The thick solid lines refer to our reference case, which lie between the two extreme scenarios. Fig. 4 illustrates our conservative bounds (solid thick lines), together with the existing constraints from VOYAGER 1 $e^{\pm}$ data [2] (dashed green and blue lines), from a compilation of X-ray and γ-ray data [3] (dot-dashed green line), from the CMB assuming s-wave [4, 5] (dotted green and blue lines in the lower portion of the plot) or p-wave annihilation [6, 7] (dotted green and blue lines in the upper portion of the plot). For each probe, each colour denotes a specific annihilation channel: green for $\chi\chi \to e^+e^-$, blue for $\chi\chi \to \mu^+\mu^-$ and magenta for $\chi\chi \to \pi^+\pi^-$. At the time of writing, we are the only ones who have derived constrains on the $\pi^+\pi^-$ channel from sub-GeV DM.

4. Conclusion

We derive the constraints on $\langle\sigma v\rangle$ for dark matter particles with a mass from 1 MeV up to 5 GeV, annihilating via three channels: electron, muon and pion. We adopted the data from the INTEGRAL/SPI detector. If the DM annihilation cross section is a p−wave, our bounds are the most stringent for 150 MeV $\leq m_\chi \leq$ 1.5 GeV. Our constraints can be improved by 60% by including an astrophysical contribution.

5. Acknowledgements

E.P. acknowledges support from the research grant "Bando Vinci 2020", funded by the Università Italo-Francese.

References

[1] M. Cirelli, N. Fornengo, B. J. Kavanagh and E. Pinetti, *Integral X-ray constraints on sub-GeV Dark Matter*, *Phys. Rev. D* **103** (2021) 063022 [2007.11493].

[2] M. Boudaud, J. Lavalle and P. Salati, *Novel cosmic-ray electron and positron constraints on MeV dark matter particles*, *Phys. Rev. Lett.* **119** (2017) 021103 [1612.07698].

[3] R. Essig, E. Kuflik, S. D. McDermott, T. Volansky and K. M. Zurek, *Constraining Light Dark Matter with Diffuse X-Ray and Gamma-Ray Observations*, *JHEP* **11** (2013) 193 [1309.4091].

[4] T. R. Slatyer, *Indirect dark matter signatures in the cosmic dark ages. I. Generalizing the bound on s-wave dark matter annihilation from Planck results*, *Phys. Rev. D* **93** (2016) 023527 [1506.03811].

[5] L. Lopez-Honorez, O. Mena, S. Palomares-Ruiz and A. C. Vincent, *Constraints on dark matter annihilation from CMB observationsbefore Planck*, *JCAP* **07** (2013) 046 [1303.5094].

[6] R. Diamanti, L. Lopez-Honorez, O. Mena, S. Palomares-Ruiz and A. C. Vincent, *Constraining Dark Matter Late-Time Energy Injection: Decays and P-Wave Annihilations*, *JCAP* **02** (2014) 017 [1308.2578].

[7] H. Liu, W. Qin, G. W. Ridgway and T. R. Slatyer, *Lyman-α Constraints on Cosmic Heating from Dark Matter Annihilation and Decay*, 2008.01084.

[8] J. Buch, M. Cirelli, G. Giesen and M. Taoso, *PPPC 4 DM secondary: A Poor Particle Physicist Cookbook for secondary radiation from Dark Matter*, *JCAP* **09** (2015) 037 [1505.01049].

[9] L. Bouchet, A. W. Strong, T. A. Porter, I. V. Moskalenko, E. Jourdain and J.-P. Roques, *Diffuse emission measurement with INTEGRAL/SPI as indirect probe of cosmic-ray electrons and positrons*, *Astrophys. J.* **739** (2011) 29 [1107.0200].

[10] Fermi-LAT collaboration, *Limits on Dark Matter Annihilation Signals from the Fermi LAT 4-year Measurement of the Isotropic Gamma-Ray Background*, *JCAP* **09** (2015) 008 [1501.05464].